Improved Detection of Iron-Loaded Cells by Combining Balanced Steady-State Free Precession (bSSFP) Imaging with Susceptibility Weighted Imaging (SWI) Processing.

F. M. Martinez-Santiesteban[1], E. J. Ribot[1], P. J. Foster[1], and B. K. Rutt[2]

[1]Robarts Research Institute, University of Western Ontario, London, Ontario, Canada, [2]Department of Radiology, Stanford University, Palo Alto, California, United States

Introduction: MR imaging of iron-loaded cells has been successfully accomplished, both *ex vivo* and *in vivo*, using the balanced steady state free precession (bSSFP) pulse sequence, with performance advantages over gradient echo (GRE) pulse sequences [1,2]. In addition, Susceptibility Weighted Imaging (SWI) has been used to enhance conventional magnitude MR images to detect small susceptibility differences with respect to normal tissue [3]. As input to the SWI processing, one generally uses a flow-compensated T2*-weighted GRE pulse sequences to create enough dephasing in regions of magnetic susceptibility change. SWI processing consists of combining both phase and magnitude images together to accentuate this susceptibility contrast, and has been shown to better reveal small susceptibility changes present in particular regions of the imaged tissue, for example venous vessels [4-8]. To the best of our knowledge, bSSFP has not previously been used as input to SWI processing because, typically, it is used with a symmetrical readout, such that TE=TR/2, giving it similar properties to a spin echo (SE) acquisition [9]. We have observed that under these circumstances, most of the dephasing produced around iron-loaded cells is refocused and therefore SWI does not provide a significant improvement over bSSFP for the detection of minute amounts of iron. When the bSSFP echo time is shifted to a value significantly greater than TR/2 (i.e. asymmetric readout), then bSSFP acquisition takes on some characteristics of a T2*-weighted GRE acquisition and additional dephasing is registered around the iron loaded cells. Once that additional phase information is available, then SWI techniques can be used to further enhance the magnitude images acquired with bSSFP.

Methods: *Animal Model:* Brain metastatic breast cancer cells (MDA-MB-231BR) were labelled with micron-sized particle iron oxide (MPIO, 0.9μm diameter) and injected into the left heart ventricle of nude mice. At 29 days post-injection, when single labelled cells were still present along with developing brain metastases, mice were sacrificed after ex-sanguination and perfusion fixed using 4% formalin. The brains were then removed and placed in formalin for 48h. For imaging purposes, the brains were placed in 1-cm-diameter plastic tubes immersed in Fluorinert (3M, Minneapolis, MN, USA), a perfluorocarbon ether that does not have any MR signal. *Magnetic Resonance Imaging:* All MRI examinations were performed on a 1.5T whole-body clinical MR scanner using a custom-built gradient coil (inner diameter=17cm; maximum gradient strength=500mT/m; peak slew rate=2000T/m/s). Mice were imaged using a custom-built solenoid mouse head radiofrequency coil (inner diameter=1.5cm). Imaging parameters were previously optimized for the simultaneous detection of metastatic tumours and iron-loaded cells and they are as follows: 3D bSSFP, resolution=100x100x200μm, 2 averages, 4 phase cycles, TR=26 ms, TE=13 ms, rBW=42 kHz, and 35º flip angle [10]. For asymmetric SWI-bSSFP, TE was increased to 21 ms keeping all the other parameters constant. The images of each phase cycle were stored for further SWI processing and the final magnitude bSSFP images were obtained using the sum of squares (SOS) of all the phase cycles [11]. *Image Processing:* 2D SWI procedures using positive, negative, and triangular phase masks were used for each phase-cycled image of both bSSFP acquisitions (TE=TR/2 and TE>TR/2). For all the experiments, a multiplication factor q=3 and a homodyne filter with cut-off frequency of 25% of the maximum spatial frequency were used [2,4-8]. The final magnitude SW images were obtained using the SOS over the phase cycles and then obtaining the minimum intensity projection (mIP) over the three SWI methods, i.e. positive, negative, and triangular phase masks. The fractional signal loss (ΔS/S), defined as (Sb-Sv)/Sb where Sv is the minimum signal intensity of the dark spots and Sb is the mean signal intensity of the surrounding tissue, was obtained over 25 different regions.

Results: Figure 1 presents a coronal image of a mouse brain using conventional bSSFP (A) and SWI-bSSFP (B). As can be seen SWI-bSSFP allows the detection of signal voids, i.e. iron-loaded cells, not detected with conventional bSSFP, as shown on the circular dotted regions. The mean values of ΔS/S were 28% for bSSFP with TE=TR/2, 36% for bSSFP with TE>TR/2, 34% for SWI-bSSFP with TE=TR/2, and 45% for SWI-bSSFP with TE>TR/2. Interestingly, SWI did not offer any enhancement of ΔS/S when applied to bSSFP with TE=TR/2 but it did increase it for the case where TE>TR/2. This can be observed in Figure 1 by noticing the well-defined and darker black spots present in (B) compared to the dimmer and blurred spots in (A). Even though the present work did not target the contrast of the metastatic tumours, it is observed that on regions without significant T2* weighting the tumours are more easily observed with SWI-bSSFP (rectangular dotted regions), whereas regions with more signal loss the tumours are less visible (arrows).

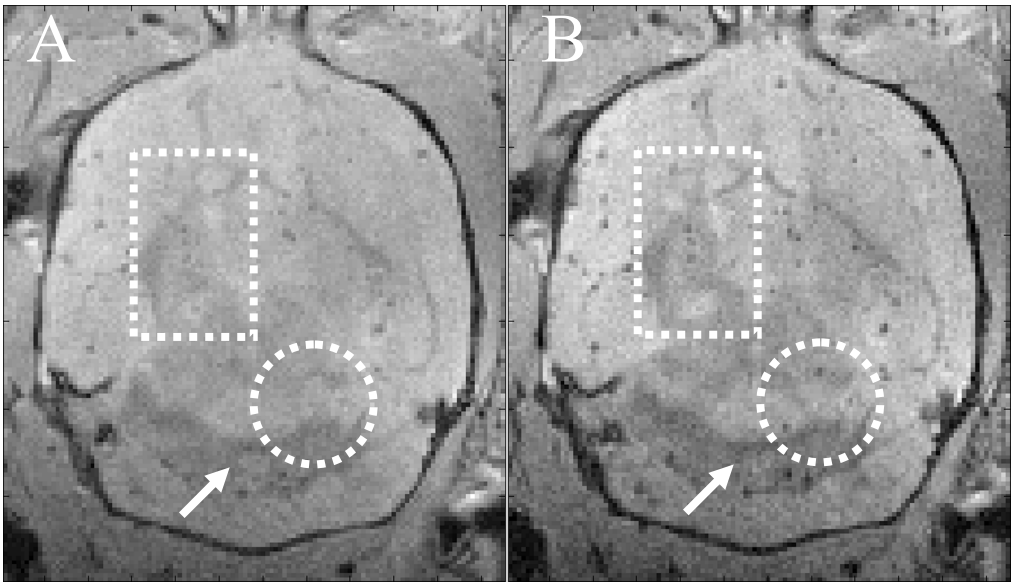

Figure 1. (A) bSSFP image with TR/TE=26/13 ms; (B) SWI-bSSFP with TR/TE=26/13 ms

Conclusions: Changing the echo time of bSSFP to a value significantly higher than TR/2 provides additional information in the phase images that can be used to enhance the contrast of susceptibility changes using SWI. Even though SWI processing generally leads to an SNR decrease, it also increases the contrast of small structures that exhibit susceptibility differences with respect to the surrounding tissue. By combining the high SNR efficiency of bSSFP and the enhanced susceptibility contrast afforded by SWI processing, the detection of iron-loaded cells is significantly improved. It is expected that the presented method would be used not only for cellular imaging, but also for the early detection of other diseases that involve susceptibility changes of sub-voxel dimensions such as amyloid-beta plaques in Alzheimer's, iron accumulation in Parkinson's disease and micro-vascular changes associated with stroke.

References: [1] Heyn et al. MRM 2006 55 (1) pp. 23-29. **[2]** Heyn et al. MRM 2006 56 (5) pp. 1001-1010. **[3]** E. Mark Haacke, et al. MRM 52:612–618 (2004). **[4]** J. R. Reichenbach, et al. J. of Comp. Assisted Tomography, vol. 24, no. 6, pp. 949–957, 2000. **[5]** Y.Wang, et al. JMRI, vol. 12, pp. 661–670, 2000. **[6]** J. R. Reichenbach et al. NMR in Biomed. vol. 14, pp. 453–467, 2001. **[7]** A. M. Abduljalil, et al. JMRI, vol. 18, pp. 284–290, 2003. **[8]** N. D. Wycliffe, et al. JMRI, vol. 20, pp. 372–377, 2004. **[9]** Klaus Scheffler et al. MRM 49:395–397 (2003). **[10]** EJ. Ribot, et al. 2009 WMIC, Sep. 23-26, 2009; Montreal, Canada. **[11]** Bangerter NK, et al. MRM 51:1038-1047 (2004).